RFI Suppression for Synchronous Impulse Reconstruction UWB Radar Using RELAX

Ode Ojowu Jr.[1], Jian Li[*2]

Department of Electrical and Computer Engineering, University of Florida, Gainesville, FL 32611, USA

[1]ojowuode@ufl.edu; [*2]li@dsp.ufl.edu

Abstract

This paper focuses on suppression of Radio Frequency Interference (RFI) for ultra-wideband (UWB) radar signals, sampled using the synchronous impulse reconstruction (SIRE) time equivalent sampling scheme. This equivalent sampling scheme is based on the Army Research Lab's (ARL) efforts to build an ultra-wideband (UWB) radar in forward looking mode that samples returned radar signals using low rate and inexpensive analog-to-digital (A/D) converters. The cost effectiveness off this SIRE UWB radar makes it plausible for actual ground missions for detecting buried explosive devices. However, the equivalent time sampling scheme complicates RFI suppression as the RFI samples are aliased and irregularly sampled in real time. In this paper, the RELAX and multi-snapshot RELAX algorithms are presented as an intermediate step to the previously proposed averaging scheme by the Army Research Laboratory, in order to enhance RFI suppression for this sampling scheme. The proposed suppression technique involves modelling the narrowband RFI signals as a sum of sinusoids and applying the aforementioned algorithms. The RELAX algorithm improves the RFI suppression performance without altering the target signatures compared to AR modelling. The multi-snapshot RELAX algorithm which provides a more accurate sinusoidal model than the RELAX algorithm, improves on the RELAX algorithm in terms of suppression. However, the target signatures are suppressed as the number of sinusoids increases. The analysis of the algorithmsis was performed by using collected sniff (passive) data using the SIRE radar in addition to simulated wide-band echo signals (point target signatures).

Keywords

RELAX; RFI Suppression; SAR; Synchronous Impulse Reconstruction (SIRE); UWB

Introduction

Ultra-wideband (UWB) radar is a commonly used tool for various remote sensing applications. Such applications include but are not limited to the use of low frequency, high bandwidth pulses for detecting improvised explosive devices (IEDs) and land mine targets. The effective detectionof land mines and other IEDs could lead to increased safety for various ground [1] related missions [15]. The use of low frequencies in UWB radar is necessary forfoliage or ground penetration, whereas the use of wideband pulsesis necessary for good resolution (ability to detecttar gets from clutter) [16]. However, because of these requirements, the data (target returns) collected by the UWB radar will be corrupted by signals in the radio frequency spectrum (specifically the UHF/VHF bands). These signals include FM Radio, TV broadcasts and other narrowband and wideband communication signals. The ability to effectively detect targetsis reduced by the presence of these radio frequency signals.

General methods of suppressing RFI and their limitations are discussed in detail in [16] for conventional UWB radar, which is the case when the returned signals are sampled regularly at or above the Nyquist rate.

Due to the large bandwidth of the returned radar signals, conventional sampling will require high rate analog-to-digital (A/D) converters to digitize the returned signals. These highspeed A/D converters are expensive to build and makepractical applications improbable. In order to improve the cost of UWB radars, the Army Research Laboratory (ARL) is currently working on an equivalent time sampling UWB radarin forward looking mode, referred to as the Synchronous Impulse Reconstruction (SIRE) radar [8]. This radar uses low rate (inexpensive and commercially available) A/D converters to sample the returned signals (approximately 3GHz bandwidth), which makes the radar more feasible for adoption in practice.

This material is based upon work supported by, or in part by, the U.S. Army Research Laboratory and the U.S. Army Research Office under contract/grant No. W911NF-11-2-0039. The views and conclusions contained herein are those of the authors and should not be interpreted as necessarily representing the official policies or endorsements, either expressed or implied, of the U.S. Government. The U.S. Government is authorized to reproduce and distribute reprints for Governmental purposes notwithstanding any copyright thereon.

Ode Ojowu Jr. and Jian Li are with the Department of Electrical and Computer Engineering, University of Florida, Gainesville, FL 32611-6130 USA (e-mail: ojowuode@ufl.edu; li@dsp.ufl.edu).

This equivalent time sampling scheme takes advantage of the fact that the scene is not changing with time, hence aliasing of the returned target signals can be prevented. However, this is not the case with the radio frequency signals which are changing with time. Aliasing and the irregular sampling caused by the time-equivalent scheme becomes an issue when it comes to the subject of RFI suppression as discussed in the next two sections.

This paper focuses on suppression of RFI signals for this equivalent time-sampling scheme. The goal is to model the narrowband interference as a sum of sinusoids in real timeand estimate and subtract the sinusoids before averaging to achieve further suppression.

A cyclic optimization algorithm known as RELAX [6] is proposed for estimating the parameters of the sinusoids (in an iterative manner). This algorithm is an asymptotic maximum likelihood approach [17] and is computationally and conceptually simple. It has been applied to problems like noncomtactvital sign detection for more accurate estimates of respiratory rates and heart rates [2]. It has also been shown to estimate the parameters of sinusoids accurately even in the presence of colored noise [17]. The multi-snapshot RELAX [5] algorithm, which is an extension of the RELAX algorithm, will be used to provide a more accurate sinusoidal model for the SIRE sampling scheme.

The RELAX algorithm or multi-snapshot RELAX is implemented as an intermediate step to the already proposed averaging method [9] to achieve further suppression.

In Section 2, the time equivalent SIRE sampling scheme is described. Section 3 briefly describes the limitations of some conventional methods to the SIRE sampled data for RFI suppression. The averaging method proposed in [9] for RFI suppression of SIRE sampled data is also discussed in this section, along with its performance. In Section 4, the RELAX algorithm, along with a fast computation of the spectrum of irregularly sampled SIRE data for this algorithm is presented; the multi-snapshot RELAX algorithm is also described in this section. The results are presented in Section 5, starting with simulations that show how the RELAX algorithm suppresses aliased sinusoids for simulated data. The ”sniff” (passive data collected using the SIRE UWB radar) is then used to test the effectiveness of the proposed algorithms which are compared to AR modelling of the interference based on this sampling scheme (see Appendix). Finally, the conclusions of the paper are presented in Section 6.

Notation: Boldface lower-case letters are used to denote vectors. See Table 1 for more details on notation.

TABLE 1NOTATIONS

$\mathbf{y}$	a vector
$(\cdot)^H$	conjugate transpose of a matrix or vector
$(\cdot)^T$	transpose of a matrix or vector
$\|\cdot\|$	$\ell_2$norm
$\hat{y}$	Estimate of scalar y
$\triangleq$	Definition

SIRE Equivalent Sampling Scheme

In this section, the Synchronous Impulse Reconstruction (SIRE) equivalent time sampling technique as detailed in [8] is briefly described. This time equivalent sampling scheme poses some challenges on identifying and hence suppressing RFI sources, due to the fact that the RFI sources are changing with time as will be discussed.

The SIRE sampling scheme involves sampling the returned radar signals from a scene at a significantly lower sampling rate f_s; (with corresponding sampling period Δ_s), than the Nyquist rate, which leads to aliased samples. N aliased samples are collected per pulse repetition interval (PRI) or fast time, and for each subsequent PRI, N more samples are collected with the range profile shifted byΔ_e(in time). After K pulse repetition intervals (PRIs) or slow time, a total of $K\times N$ aliased samples are collected. These samples are interleaved as shown in Fig. 1, which gives an effective sampling rate of$f_e = 1/\Delta_e$ that is equal to, or greater than the Nyquist rate. Because the scene of interest is not changing with time, the returned samples from a given range bin theoretically should also remain unchanged in time. Therefore, the interleaved samples are theoretically effectively sampled above the Nyquist rate and should be unaliased.

The measurements from each range profile are typically repeated M times and added coherently to improve the signal-to-noise ratio (SNR). Fig. 1 shows the special case of M = 1.Table 2 summarizes the parameters used by ARL in the SIRE radar pertaining to RFI suppression.

The RFI signals, which are collected in addition to the desired target returns, on the other hand, are changing with time. Therefore, when the collected data are interleaved, they do not represent the true time samples of the RFI signals.

TABLE 2ARLPARAMETERS FOR SIRE RADAR. [8]

Radar A/D sampling rate	f_s = 40 MHz
Radar A/D sampling period	Δ_s = 25 ns
Pulse repetition frequency	PRF = 1 MHz
Pulse repetition interval	PRI = 1μs
Number of range profiles	N = 7
Interleaving factor	K = 193
Total number of range profiles	$K \times N$ = 1351
Effective sampling period	f_e = 129.53 ps
Effective sampling rate	Δ_e = 7.72 GHz

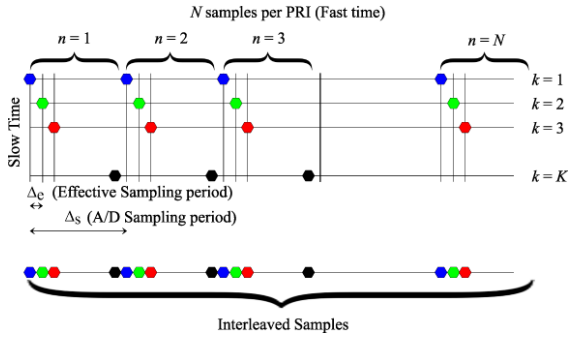

FIG. 1 SYNCHRONOUS IMPULSE RECONSTRUCTION EQUIVALENT TIME SAMPLING

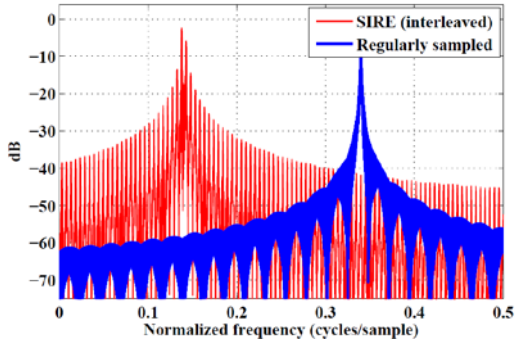

FIG. 2 SPECTRUM OF SIRE SAMPLED COMPLEX SINUSOID AFTER INTERLEAVING COMPARED TO THE SPECTRUM OF REGULARLY SAMPLED COMPLEX SINUSOID ABOVE THE NYQUIST RATE

For instance, consider a complex sinusoid sampled at f_e(see Tab. 2), with time samples $h[n] = e^{-j\omega_o n}$. The periodogram estimate of the spectrum of $h[n]$ is given by$\phi(\omega) = |(1\backslash L)H(\omega)|^2$, where

$$\sum_{n=1}^{L} H(\omega) = e^{-j\omega n} \qquad (1)$$

is the discrete-time Fourier transform (DTFT) of $h[n]$ and $L = K \times N$ is the total number of samples. If this complex sinusoid is sampled using the SIRE technique (M = 1), the time samples of the interleaved signal will be given by:

$$h[l] = \begin{Bmatrix} h[l(T+1)] \text{for } l = 0,1,\dots K \\ h[(l-K)(T+1)+K] \text{for } l = 0,1,\dots 2K \\ \dots \\ h[(l-6K)(T+1)+6K] \text{for } l = 0,1,\dots 2K \end{Bmatrix}$$

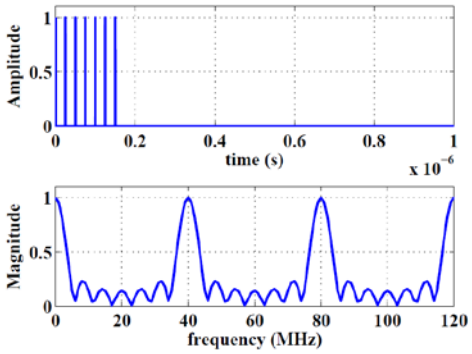

FIG. 3 SPECTRUM SIRE SAMPLING PATTERN: ONE FAST TIME PULSE (N = 7) SAMPLES

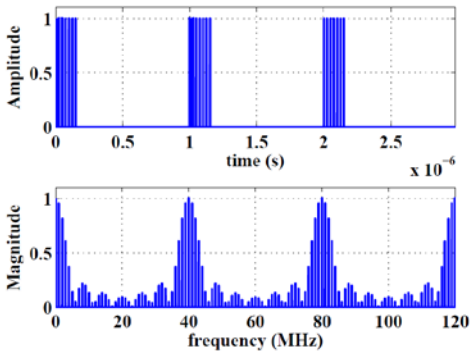

FIG. 4 PECTRUM SIRE SAMPLING PATTERN ($N \times K$ = 1351 *samples*)

Where $T = (f_e/PRF)$ (the other variables are described in Table 2). The corresponding periodogram is given by $\tilde{\phi}(\omega) = |(1\backslash L)\tilde{H}(\omega)|^2$, where $\tilde{H}(\omega)$is the DTFT of $\tilde{h}[l]$ and can be simplified to:

$$\tilde{H}(\omega) = \left(\sum_{s=0}^{6} e^{j(\omega_o-\omega)sK}\right)\left(\sum_{r=0}^{K-1} e^{j(\omega_o(T+1)-\omega)r}\right) \qquad (2)$$

Fig. 2 shows the periodogram spectral estimate of the regularly sampled sinusoid $\phi(\omega\}$and the interleaved SIRE sampled signal $\tilde{\phi}(\omega)$. The spectrum of the omplex sinusoid is not only distorted, but it peaks at a different frequency. Note that $\tilde{H}(\omega)$ can be written as:

$$\tilde{H}(\omega) = \left(\sum_{s=0}^{6} e^{j(\omega_o-\omega)sK}\right)\left(\sum_{r=0}^{K-1} e^{j(\omega_o-\omega)r}\, e^{j\omega_o Tr}\right) \qquad (3)$$

Therefore, if $\omega_o = 2\pi m/T$, where $m \in \mathbb{Z}$ then $\tilde{H}(\omega)$ reduces to $H(\omega)$. This condition implies that the frequency (in Hz) of the complex sinusoid$f = \frac{f_e \omega_o}{2\pi} = m \times$ PRI, is an integer multiple of the pulse repetition frequency. Unless this condition is true, interleaving will lead to distortion of the complex sinusoid. A single complex sinusoid, sampled regularly below the Nyquist rate (f_s), should consist of a single peak at an ambiguous frequency in the frequency domain (ina bandwidth of fs). However, due to the irregular

sampling pattern of the SIRE sampling technique, a single sinusoid willbe seen as multiple peaks within this bandwidth.

Fig. 3 shows the SIRE sampling pattern (in real time) and its corresponding spectrum for a single fast time pulse (N samples). As expected, this will result in a sinc like function every 40 MHz (f_s) in the frequency domain. However, repeating this sampling pattern K times will correspond tosampling in the frequency domain as seen in Fig. 4. Therefore, the spectrum of a single sinusoid sampled using the SIRE sampling scheme will correspond to convolving the spectrum of this sampling scheme with that of a sinusoid resulting in multiple peaks. In the next section, we discuss some of existing algorithms for RFI suppression as well as the limitations posed by this sampling scheme, based on the analysis above.

Existing RFI Suppression Methods

One popular technique for RFI suppression based on conventional sampling involves the use of notch filters. This method involves estimating the spectrum of the corrupted signal and removing the spikes in this spectrum using a notch filter. This method works well for narrowband interference sources. However, it will introduce side-lobes in the time domain [4, 11, 14]. Filtering techniques in general, suffer from filter transients and reduced data length. The notch filtering problem is even more severe because of the ambiguity in frequency for the SIRE sampling scheme based on the analysis in the previous section and Fig. 2 for the interleaved signals. Also, if the analysis of the corrupted signal is performed in real-time (before interleaving), one interference source will appear to have multiple peaks in the spectrum due to irregular sampling as seen in Fig. 4, which makes this method not applicable.

Modelling the RFI using AR models can also be used for suppression (see Appendix). The irregular sampling of the SIRE data makes this endeavour challenging. However, the SIRE sampled data is sampled regularly in fast time and slow time, and this can be exploited for AR modelling. There are only N= 7 samples sampled regularly in fast time, whereas there are K= 193 regularly sampled samples in slow time. These slow time samples can be used for AR modelling with N= 7 snapshots allowing for more freedom in the choice of the AR model order (see Appendix for AR modelling of SIRE sampled data).

Modelling the narrowband RFI as a sum of sinusoids,

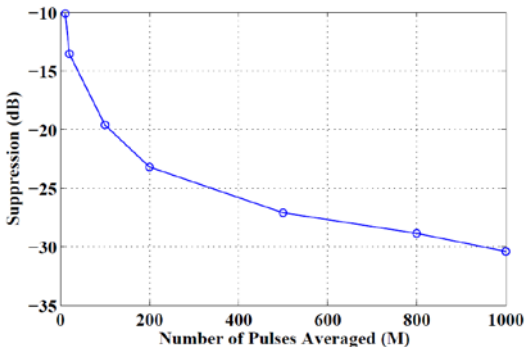

FIG. 5 RFI SUPPRESSION (dB): AVERAGINGMETHOD (Mrealizations) FOR SIMULATED SIRE SAMPLED RFI SIGNALS

and estimating their parameters have been shown to be effective for suppressing RFI with little signal distortion [12, 14]. This method involves estimating the amplitude, frequency and phase of each interfering sinusoid and subtracting the resulting sinusoid from the corrupted data. The effectiveness depends on how accurate these parameters are estimated, and reduced if the sinusoidal model for the RFI signals starts to breakdown [12]. This occurs when the duration of data is greater than the modulation time (inverse of modulation bandwidth) of the RFI signals. For instance, a 3 kHz narrowband voice channel will have a modulation time of approximately 0.3 ms, whereas wideband TV signals with bandwidth of several kHz will have a much smaller modulation time [12]. If the duration of the processed data is greater than this modulation time, the estimated parameters will change during the acquisition time, leading to less effective suppression. These methods are also computationally expensive when many interference sources are estimated. When the RFI signals are sampled using the SIRE equivalent sampling scheme, estimation of these parameters becomes even more challenging due to the irregular sampling pattern and aliasing introduced, even if the model is accurate.

Another technique for RFI suppression is using passive data to adaptively suppress RFI from active radar data by projecting the measured active data to a signal subspace created by the passive data. This method assumes orthogonality between the desired target signatures and the RFI, and has been shown to be effective for RFI suppression in [16] for conventionally sampled data. However, as noted in [3], this method is inadequate for suppression of SIRE sampled data, due to the irregular sampling pattern and aliased samples of the RFI. These challenges have prompted the need for new RFI suppression techniques for the SIRE sampling scheme.

The averaging method proposed in [9] and also

detailed therein, has been shown to suppress wideband and narrowband interferers. The method is based on repeating the measurements from the same range profile *M* times and averaging the repeated measurements. The averaged samples are then interleaved and used for generating SAR images. Fig. 5 shows the amount of suppression as a function of the number of repeated measurements based on simulated RFI sources. Asimilar plot can be seen in [9]. An important point to noteis that this method of suppression does not take into accountany properties of the RFI signal, which is the motivation for improving the performance.

In this paper, the averaging method is improved by analyzing the data in 'real-time' (before interleaving). The aliased samples of the data in 'real-time' are modelled as a sum of sinusoids, in other to achieve further suppression with little signal distortion. The parameters of the sinusoids are estimated and the resulting sinusoids are subtracted from the data using the RELAX algorithms [5, 6] (to provide accurate estimates of the parameters) before averaging.

Based on the analysis in the previous section, a single sinusoid appears as multiple peaks due to the irregular SIRE sampling pattern in 'real-time'. However, in theory, estimating the parameters of a single sinusoid from the maximum peaklocation of the spectrum, and subtracting this from the data, will correspond to its removal from the spectrum. This will eliminate all the multiple aliased peaks (Fig. 4). This analysis will be shown on simulated sinusoids in the results section.

The RELAX algorithm and its multi-snapshot counterpart are described in the next section and the steps for RFI suppression are also presented.

Proposed RFI Suppression Method: RELAX and Averaging

Modelling of RFI

The proposed suppression method, entails modelling RFI signals of length L collected in real time (before interleaving) as a sum of P complex-valued aliased sinusoids as described in Eq. (4):

$$\mathbf{z} = \sum_{p=1}^{P} \alpha_p \mathbf{a}(f_p) \tag{4}$$

Where α_p and f_p are the complex amplitude and frequency of the *p*th sinusoid and

$$\mathbf{a}(f_p) = \begin{bmatrix} 1 & e^{j2\pi f_p} & \cdots & e^{j2\pi f_p (L-1)} \end{bmatrix}^T$$

The received measurement signal can be written as $\mathbf{y} = \mathbf{z} + \mathbf{s} + \mathbf{n}$, where $\mathbf{z}$, $\mathbf{s}$, and $\mathbf{n}$, are the RFI signal, desired target returns, and receiver noise, respectively. The target returns have a wide bandwidth relative to the RFI signals and can be modelled as white noise [3, 16]. RFI suppression, then, becomes a case of estimating the parameters of multiple sinusoids in the presence of white noise. The non-linear least squares (NLS) approach (an asymptotic Maximum Likelihood approach [17, 18]) estimates these parameters by minimizing the following non-linear least squares cost function in Eq. (5).

$$\{\hat{\alpha}_p, \hat{f}_p\}_{p=1}^{P} = \underbrace{\operatorname{argmin}}_{\{\alpha_p, f_p\}_{p=1}^{P}} \left\| \mathbf{y} - \sum_{p=1}^{P} \alpha_p \mathbf{a}(f_p) \right\|^2 \tag{5}$$

Where *P* is the number of sinusoids, which can be estimated using a model-order selection tool like the Bayesian Information Criterion (BIC) [19]. This method can approach the Cramer-Rao bound in performance, but it involves a multidimensional search and hence involves complex computations for the case of multiple sinusoids. It can also be sensitive toinitializations [18, 20]. The RELAX algorithm can be used for solving the problem in an iterative manner reducing the computational complexity significantly [6]. This conceptually and computationally simple algorithm was shown to estimate sinusoidal parameters accurately and robustly even in the presence of colored noise [17]. The parameters are estimated for the above non-linear least squares fitting problem in an iterative manner as described below.

RELAX Algorithm

The RELAX algorithm estimates the parameters as follows: Let

$$\mathbf{y}_{\mathrm{p}} \triangleq \mathbf{y} - \sum_{i=1, p\neq i}^{P} \hat{\alpha}_i \mathbf{a}(\hat{f}_i) \tag{6}$$

The frequency and complex, amplitude estimates of the *p*th sinusoid are, respectively, estimated by:

$$\hat{f}_p = \underbrace{\operatorname{argmax}}_{f_p} \left| \mathbf{a}^H(f_p) \mathbf{y}_p \right|^2 \tag{7}$$

and

$$\hat{\alpha}_p = \underbrace{\frac{\mathbf{a}^H(f_p)\mathbf{y}_p}{L}}_{\text{DTFT of } \mathbf{y}_p} \Bigg|_{f_p = \hat{f}_p} \tag{8}$$

The RELAX algorithm steps are given by:

- Step 1: Assume *P*= 1. Estimate $\hat{f}_1$ and $\hat{\alpha}_1$ from $\mathbf{y}$.

- Step 2: Assume P= 2. Compute $\mathbf{y}_2$ based on estimates from the previous step and estimate $\hat{f}_2$ and $\hat{\alpha}_2$. Compute $\mathbf{y}_1$ and re-estimate $\widehat{f}_1$ and $\widehat{\alpha}_1$. Re-iterate previous steps until practical convergence.
- Step 3: Assume P= 3. Compute $\mathbf{y}_3$and estimate $\hat{f}_3$ and $\hat{\alpha}_3$. Re-compute $\mathbf{y}_1$ and re-estimate $\hat{f}_1$ and $\widehat{\alpha}_1$ from $\hat{f}_2$, $\hat{\alpha}_2$, $\hat{f}_3$ and $\hat{\alpha}_3$. Re-iterate until convergence or a fixed number of iterations.
- Remaining Steps: Continue until$P = \hat{P}$, which is an estimated or desired number.

Note that, the frequencies and complex amplitudes in (7) and (8), respectively, are estimated using the DTFT of the signals $\mathbf{y}_p$. This can be efficiently computed using the FFTand zero-padding for conventionally (regularly) sampled data.

Based on Fig. 3 and the analysis leading to Eq. (3), as previously discussed, the interleaving process of a SIRE sampled sinusoid leads to a distortion of that signal except for a specific case, being that the frequency of the sinusoid isan integer multiple of the PRI. The analysis of the RFI using the RELAX algorithm will, therefore, be performed on the data in real-time (before the interleaving process). As it will be shown in the results section, the estimated complex amplitudes and frequencies (although possibly ambiguous), can be used to accurately reconstruct the aliased RFI samples and yield effective RFI suppression using the RELAX algorithm.

The RELAX algorithm requires the computation of the spectrum of the received samples. For irregularly sampled SIRE data, this spectrum can be computed using an FFT afterre-sampling data (interpolating with zeros). Re-sampling this data to give a regularly sampled data with effective sampling frequency of f_e, will lead to a significantly long datasequence with most of the samples being zero. For instance, one realization ($M = 1$) of a SIRE sampled data, sampled at $f_s = 40$MHz , contains $N = 7$ aliased samples per PRI. After re-sampling to an effective rate of $f_e = 7.72$ GHz, each PRI will consist of $T = f_e \times \text{PRI} = 7720$ samples. Hence a total of $T \times K = 7720 \times 193 \approx 1.5$ million samples per realization. Therefore, applying a direct FFT (with zeropadding) to this re-sampled data to estimate the frequencies and complex amplitudes becomes computationally intensive with a computational complexity of $\mathcal{O}(TK\log TK)$.

Note that similar to Fig. 4, a single sinusoid sampled usingthe SIRE sampling technique and re-sampled as discussed above to give an effective sampling rate of $f_e = 7.72$GHz will repeat itself approximately every 40MHz (A/D rate) in the frequency domain, due to aliasing. In order to reduce the computational complexity of this re-sampling scheme, the regular sampling of the data in both fast and slow time can be exploited and the spectrum can be computed only on a40 MHz bandwidth to save on computations. The analysis is performed as follows: The spectral estimate for SIRE sampled data in real time (before interleaving) based on parameters in Tab. 2 is given by:

$$X(f) = \sum_n \sum_m x_{m,n} e^{-j2\pi f(m\Delta_m + n\Delta_n)} \quad (9)$$

where

$n = 0, 1, 2, \cdots, N-1$ $(N = 7)$
$m = 0, 1, 2, \cdots, K-1$ $(K = 193)$
$\Delta_n = \Delta_s = 25$ ns, (ADC sampling rate),
$\Delta_m = \text{PRI} + \Delta_e$

A direct computation of the spectrum in Eq. (9) is obviously computationally intensive, especially for a fine grid size infrequency. Assuming

$$f = \frac{k_1}{\Delta_m} + k_2\Delta_f \quad (10)$$

where

$k_1 = 0, 1, 2, \cdots, K_1 - 1 \quad K_1 = T = 7720$
$k_2 = 0, 1, 2, \cdots, K_2 - 1 \quad K_2 = 1/(\Delta_m \Delta_f)$
$\Delta_f =$ fixed grid size (in Hz)

Eq. (10) is the frequency grid (in Hz) on which the spectrum in Eq. (9) will be computed. Note that the choice of K_2 determines the grid spacing Δ_f and the choice of the k_1 values determines the portion of the bandwidth in which the spectrum is to be estimated.

For instance, $k_1 = 0,1,\cdots, T = 7720$ computes the spectrum over the entire 7.72 GHz (effective sampling rate) bandwidth. For the frequency grid specified in (10), the spectrum in(9) can be re-written as follows:

$$X(f) = \sum_n \sum_m x_{m,n} e^{-j2\pi\left(\frac{k_1}{\Delta_m} + k_2\Delta_f\right)(m\Delta_m + n\Delta_n)} \quad (11)$$

which simplifies to:

$$X(k_1, k_2) = \sum_n x_{m,n} e^{-j2\pi\left(\frac{k_1}{\Delta_m} + k_2\Delta_f\right)n\Delta_n} \sum_m x_{m,n} e^{-j2\pi\left(\frac{k_2}{K}\right)m}$$

$$X(k_1, k_2) = \sum_n x_{m,n} e^{-j2\pi\left(\frac{k_1}{\Delta_m} + k_2\Delta_f\right)n\Delta_n} X_n(k_2) \quad (12)$$

From Eq. (12), the spectrum is computed by summing upmultiple FFTs. Also because the signal is aliased, the spectrumneeds only to be computed over a small portion (40 MHz -A/D sampling rate) of the entire bandwidth. The computational complexity of this algorithm is $\mathcal{O}(NK_2\log K_2 + K_1K_2N)$. Note that the bottle neck of this algorithm is in the second term. When the

TABLE 3SUPPRESSION ALGORITHM: RELAX + AVERAGING

Step 1:	RELAX (*P* sinusoids estimated).
	- Compute the DTFT of the measured data (**y**)from (12) and estimate $\hat{f}_1$ and $\hat{a}_1$ using (7) and (8).
	- Compute $\mathbf{y}_2$using (6) and its DTFT using (12). Estimate $\hat{f}_2$ and $\hat{a}_2$ using. Re-estimate $\hat{f}_1$ and $\hat{a}_1$from $\mathbf{y}_1$ and iterate. Continue for $\mathbf{y}_p$, $\hat{f}_p$ and $\hat{a}_p$ $(3 \le p \le P)$ (Section 4.B).
Step 2:	Reconstruct aliased RFI samples using $\{\hat{f}_p\}_{p=1}^{P}$ and $\{\hat{a}_p\}_{p=1}^{P}$ from each realization (**y**). Subtract from each realization of (**y**)
Step 3:	Average residue from each realization and interleave.

spectrum is computed over the entire frequency grid, $K_1 = T = 7720$, the computational complexity is on the same order as re-sampling and applying an FFT. However, when the spectrum is computed over a 40 MHz bandwidth ($K_1 = 40$), this algorithm drastically improves on the computation. For example, for a frequency grid withspacing (Δ_f) of approximately 2 kHz, the spectrum in Fig.4 was computed in **0.26**secs when the SIRE sampled data was re-sampled and the FFT was applied directly using theMATLAB software. However, the spectrum based on Eq. (12) was computed in **0.035**secs on a 40 MHz grid. This spectrum is used in the RELAX algorithm (7) and (8), to estimate the parameters of the sinusoids present. The RELAX algorithm is applied here to one realization ($M = 1$) of SIRE sampled data (which correspond to a data with an acquisition time of 0.193ms based on Tab. 2). Therefore a narrowband interference source with a modulation bandwidth of 5 kHz or less can be accurately approximated as a single tone, whereas multiple sinusoids are needed to model an interference source with widerband width. The sinusoidal model begins to break down for very wideband interferers. In the next subsection we propose the multi-snapshot RELAX algorithm for SIRE sampled data that provides a more accurate sinusoidal model for the RFI signals by using fewer samples (smaller modulation time), for suppression. The overall proposed RFI suppression algorithm can be summarized in the following steps as shown in Tab. 3for RELAX.

Multi-snapshot RELAX algorithm

The multi-snapshot RELAX algorithm [5] uses $N = 7$ samples (150 ns acquisition time) for RFI suppression. Interference sources with modulation bandwidth of 6.7 MHz or less can be accurately modelled as sinusoids, which includes wideband interferers like TV broadcasts etc.

The multi-snapshot RELAX algorithm (M-RELAX forshort) proposed for angle and waveform estimation in [5] is amodification of the originally proposed RELAX algorithm [6]. The algorithm estimates the angle of arrival (using multiplesnapshots of the data) and the corresponding waveform for each snapshot.

This algorithm is proposed here for RFI suppression of SIRE sampled data to provide a more accurate sinusoidal model for the RFI signals. Here, each set of *N*= 7 fasttime samples is treated as a snapshot. The data is split into*K*= 193 total snapshots based on the parameters in Tab. 2. The frequency of a single tone is estimated by averaging the periodogram of each snapshot and finding the frequency that maximizes the average. The complex amplitudes of each snapshot is estimated by finding the complex value of the spectrum of each snapshot at the estimated frequency. Note that for a single complex sinusoid, *K*= 193 complex amplitudes are estimated from each snapshot, whereas only one frequency is estimated.

The parameters are estimated asgiven in Eq. (13) (modification of NLS for the multi-snapshotcase [5]):

$$\{\hat{\boldsymbol{a}}_p, \hat{f}_p\}_{p=1}^{P} = \underbrace{\operatorname{argmin}}_{\{\boldsymbol{a}_p, f_p\}_{p=1}^{P}} \sum_{m=1}^{K} \left\| \mathbf{x}(m) - \sum_{p=1}^{P} \alpha_p(\mathrm{k})\mathbf{a}(f_p) \right\|^2 \tag{13}$$

TABLE 4 SUPPRESSION ALGORITHM: M-RELAX + AVERAGING

Step 1:	M-RELAX (*P* sinusoids estimated).
	- Compute the DTFT of the mth snapshot of the measured data($\mathbf{x}(m)$)from (19) and estimate $\hat{f}_1$ and $\hat{a}_1(m)$ using (15) and (16).
	- Compute $\mathbf{x}_2(m)$using (14) and its DTFT using (19). Estimate $\hat{f}_2$and $\hat{a}_2(m)$. Re-estimate $\hat{f}_1$ and $\hat{a}_1(m)$from $\mathbf{x}_1(m)$ and iterate. Continue for $\mathbf{x}_p(m)$, $\hat{f}_p$ and $\hat{a}_p(m)$ $(3 \le p \le P)$ (Section 4.C).
Step 2:	Reconstruct aliased RFI samples using $\{\hat{f}_p\}_{p=1}^{P}$ and $\{\hat{a}_p(m)\}_{p=1}^{P}$ Subtract from each realization (**y**)
Step 3:	Average residue from each realization and interleave.

where $\boldsymbol{a}_p = [\alpha_p(1), \alpha_p(2), \cdots, \alpha_p(K)]$ contains the estimated complex amplitudes of the pth sinusoid for each of the K snapshots, $\hat{f}_p$ is the estimated frequency of the pth sinusoid forall snapshots and $\mathbf{x}(m)$is the mth snapshot. These parametersare estimated as follows. Let

$$\mathbf{x}_p(m) \triangleq \mathbf{x}(m) - \sum_{i=1, p\neq i}^{P} \hat{\alpha}_i(\mathrm{m})\mathbf{a}(\hat{f}_i) \qquad (14)$$

The estimates described above are given by

$$\hat{f}_p = \underbrace{\operatorname{argmax}}_{f_p} \sum_{m=1}^{K} \left|\mathbf{a}^H(f_p)\mathbf{x}_p(m)\right|^2 \qquad (15)$$

and

$$\hat{\alpha}_p(m) = \underbrace{\frac{\mathbf{a}^H(f_p)\mathbf{x}_p(m)}{N}}_{\text{DTFT of } \mathbf{x}_p(m)}\Bigg|_{f_p=\hat{f}_p} \quad m = 1,2,\dots,K \qquad (16)$$

The multi-snapshot RELAX algorithm steps are as follows:

- Step 1: Assume P= 1. Estimate $\hat{f}_1$ and $\hat{\alpha}_1(m)$ from $\mathbf{x}(m)$, for $m = 1,2,\dots,K$.
- Step 2: Assume P= 2. Compute $\mathbf{x}_2(m)$ based on estimates from the previous step and estimate $\hat{f}_2$ and $\hat{\alpha}_2(m)$, for $m = 1,2,\dots,K$. Compute $\mathbf{x}_1(m)$ and re-estimate $\hat{f}_1$ and $\hat{\alpha}_1(m)$, for $m = 1,2,\dots,K$. Re-iterate previous steps until convergence.
- Step 3: Assume P= 3. Compute $\mathbf{x}_3(m)$ using $\{\hat{\boldsymbol{a}}_p, \hat{f}_p\}_{p=1,2}$ and estimate $\hat{f}_3$ and $\hat{\alpha}_3(m)$, for $m = 1,2,\dots,K$. Re-compute $\mathbf{x}_1(m)$ and re-estimate $\hat{f}_1$ and $\hat{\alpha}_1(m)$ from $\{\hat{\boldsymbol{a}}_p, \hat{f}_p\}_{p=2,3}$ for $m = 1,2,\dots,K$. Then re-compute $\mathbf{x}_2(m)$ and re-estimate $\hat{f}_2$ and $\hat{\alpha}_2(m)$ from $\{\hat{\boldsymbol{a}}_p, \hat{f}_p\}_{p=1,3}$ for $m = 1,2,\dots,K$. Re-iterate until convergence or a fixed number of iterations.
- Remaining Steps: Continue until$P = \hat{P}$, which is an estimated or desired number.

For the SIRE sampled data, the spectrum (DTFT) of each snapshot can be described as follows. Let $\mathbf{x}(m) = \{d_m(n)\}_{n=0}^{N-1=6}$ correspond to the mth snapshot, where $d_m(n)$denotes the nth sample of the mth fast time pulse($m = 1,2,\dots,K$). Note that each snapshot is regularly sampled (at the A/D rate). The spectral estimate can therefore be computed using an FFT multiplied by a corresponding phase shift (overa 40 MHz bandwidth). The spectrum of each snapshot is given by:

$$X_m(f) = \sum_{n=0}^{6} d_m(n)e^{-j2\pi f(m\Delta_m + n\Delta_n)} \qquad (17)$$

Where $f \in (0, fs)$ is the frequency (in Hz), $\Delta_n = 1/f_s$ and Δ_m are the sampling period and the time difference from one snapshot to the next, respectively. Equation (18) above can be simplified as follows:

$$X_m(f) = e^{-j2\pi f(m\Delta_m)} \sum_{n=0}^{6} d_m(n)e^{-j2\pi\frac{f}{f_s}n} \qquad (18)$$

which is simplified to

$$X_m(r) = e^{-j2\pi\frac{r}{R}\left(\frac{m\Delta_m}{\Delta_n}\right)} \sum_{n=0}^{6} d_m(n)e^{-j2\pi\frac{r}{R}n} \qquad (19)$$

for a discrete frequency grid $r = 0,1,\dots,R-1$. It is important to note that parameter identifiability (maximum number of sinusoids that can be uniquely identified) [1, 7, 13], becomes an issue with this approach. Given $N = 7$ real valued samples, only upto $P = 2$ sinusoids (amplitude, frequency, and phase), can be uniquely identified. Estimating more than $P = 2$ sinusoids will significantly distort the target signatures. The overall proposed RFI suppression algorithm can be summarized in the steps as shown in Tab. 4 for multi-snapshot RELAX.

Numerical Results

Simulations

In this section, a signal consisting of three sinusoids in white noise (SNR = 10dB) is simulated and sampled using the SIRE equivalent scheme based on the parameters in Tab. 2, without repeated measurements (M= 1). The sinusoidshave frequencies $f_1 = 111.111$ MHz, $f_2 = 300$ MHzand $f_3 = 650.255$ MHz, all with amplitudes of 1. Note that the obtained samples will also correspond to a signal containing sinusoids with frequencies $f_{a1} = f_1 mod\, f_s$, $f_{a2} = f_2\, mod\, f_s$ and $f_{a3} = f_3 mod\, f_s$, as well as a signal containing sinusoids $f_{a1} + kf_s$, $f_{a2} + kf_s$ and $f_{a3} + kf_s$(where $k \in \mathbb{Z}$and $f_s$is the A/D rate). This ambiguity infrequency is caused by aliasing due to the low A/D rate of the radar. The RELAX algorithm can be used to accurately estimate the complex amplitudes of these sinusoids as wellas the ambiguous frequencies. This is achieved using the spectrum in (12) estimated only on a 40 MHz bandwidth to save on computations. The estimated parameters are then used to reconstruct the aliased samples, in order to suppress the sinusoids through subtraction. Fig. 6, shows the original signal, its spectrum and the progression of suppression as the number of estimated aliased parameters increases.

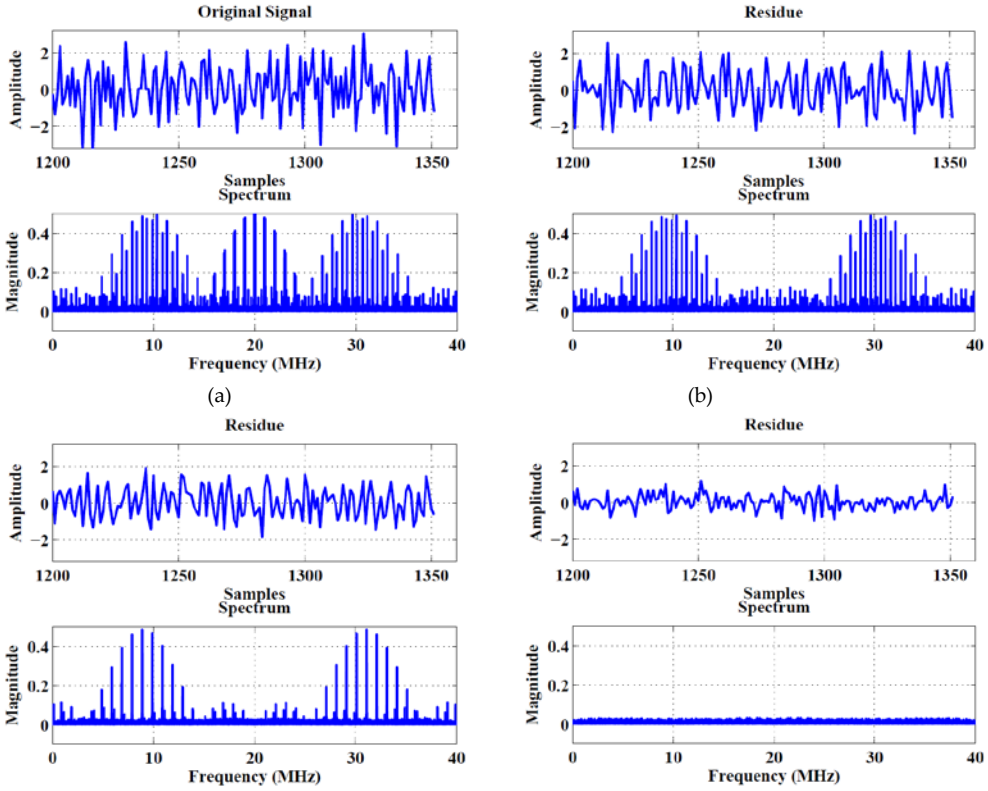

FIG. 6 RFI SUPPRESSION (SIRE SAMPLING)- SIGNAL AND SPECTRUM OF SIMULATED DATA CONTAINING 3 REAL-VALUED SINUSOIDS IN WHITE NOISE AFTER SUPPRESSION USING RELAX WITH P(REAL-VALUED) SINUSOIDSESTIMATED (a) ORIGINAL DATA (b) $P = 1$, (c) $P = 2$,(d) $P = 3$

From Fig. 6, we observe that the spectrum of the three sinusoids contains multiple peaks, due to the irregular sampling as described previously. By estimating the ambiguous frequency and complex amplitudes of each of the sinusoids (on only a40 MHz bandwidth), multiple aliased peaks are suppressed.

The purpose of the above simulations is to show the ability of the RELAX algorithm to estimate the ambiguous frequency and complex amplitudes of the sinusoids on a small bandwidth correctly, to effectively suppress the sinusoids (including the multiple aliased peaks).

In the next subsection the "sniff" dataset collected using ARL's SIRE UWB radar is analyzed and the RFI is suppressed using both the RELAX and multi-snapshot RELAX algorithms. Comparison with AR modelling of the RFI is also provided.

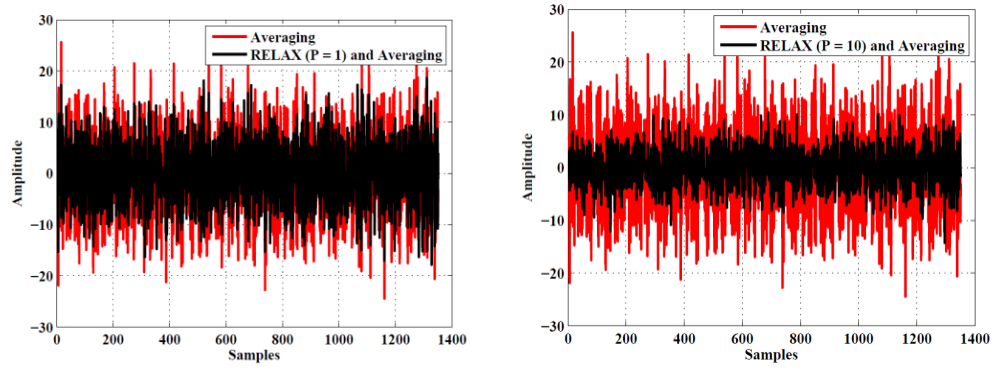

FIG. 7 RFI SUPPRESSION- RELAX ALGOTITHMSWITHP(REAL-VALUED) SINUSOIDSESTIMATEDANDSUPPRESSEDFROMSNIFF DATA (*File1*) COMPAREDTO AVERAGING (a) $P = 1$,AND (b) $P = 10$

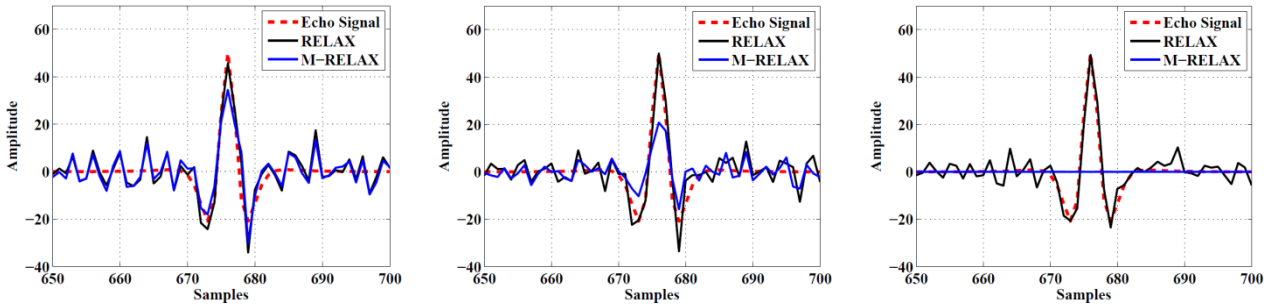

FIG. 8 ECHO RETRIEVAL (*File1*) - RELAX WITH*P*(REAL-VALUED) SINUSOIDS COMPARED TO IDEAL ECHOSIGNAL. (a) $P = 1$, (b) $P = 2$, and (c) $P = 10$.

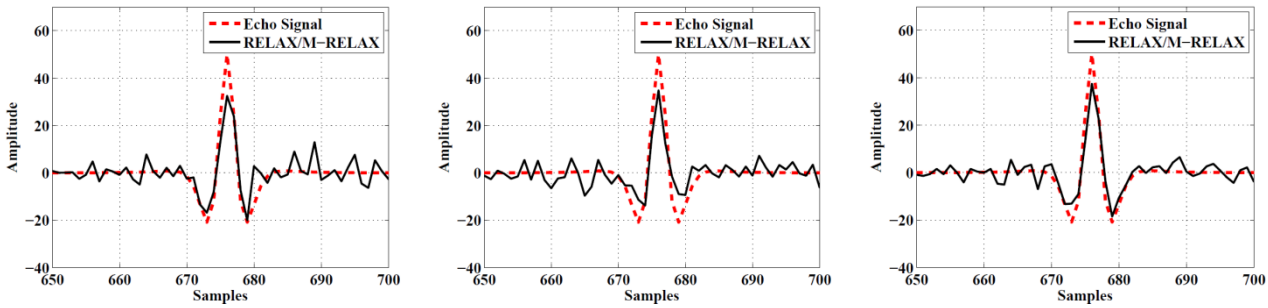

FIG. 9 ECHO RETRIEVAL (*File1*) - RELAX WITH*P* (real) SINUSOIDSCOMBINED WITH M-RELAX WITH $\tilde{P} = 1$real SINUSOIDS, COMPARED TO IDEAL ECHOSIGNAL. (a) $P = 1$, (b) $P = 2$, AND (c) $P = 10$.

"Sniff" Experimental Data

The "sniff" data to be analyzed, was collected by ARL using the SIRE UWB radar in passive mode based on the parameter sin Tab. 2. Each set of data consists of $L = K \times N = 1351$ samples. In this subsection this RFI data will be analyzed using the proposed algorithms. Two sets of RFI data with different energy levels are analyzed. For simplicity they will be referredto as *File1*and *File2*. Each set of the data, consists of *M*= 88 realizations. The amount of suppression achieved is presented in Table 5.

A wideband echo signal which represents a return froma single point target is simulated. This signal is added to each realizations (M = 88) of the "sniff" data, in a way that the echo signal adds up coherently. The goal is to show how much distortion is introduced to the desired signals after the application of the RFI suppression algorithms. Fig. 7 shows the amount of suppression achieved when the RELAX algorithm with P real-valued sinusoids is suppressed for each realization and the residues are averaged (File1). These results are compared to straightforward averaging, also in this figure.

A similar analysis is performed for the multi-snapshot RELAX algorithm and the amount of suppression can be seen in Table 5. The average power of the signals $\{\hat{s}\ (i)\}_{i=1}^{L}$, is computed using (20):

$$10\log_{10}\left(\sum_{i=1}^{L}|\hat{s}(i)|^2\right)/L \qquad (20)$$

From Table 5, it is clear that the amount of suppression increases as the number of real-valued sinusoids increases for the RELAX algorithm. This improvement comes at a cost of increased computational complexity.

TABLE 5 RFI SUPPRESSION: AVERAGE POWER COMPARISON

Signal: *File1*					
Data	Averaging	RELAX	M-RELAX	RELAX/M-RELAX($\tilde{P}=1$)	AR(order q)
39.363	18.467	15.90 ($P=1$)	15.165 ($P=1$)	12.322 ($P=1$)	16.149 ($q=2$)
		12.748 ($P=4$)	-9.579 ($P=4$)	10.248 ($P=4$)	
		11.565 ($P=7$)	-20.903 ($P=7$)	8.981 ($P=7$)	14.841 ($q=20$)
		11.302 ($P=10$)	-38.537 ($P=10$)	8.086 ($P=10$)	
Signal: *File2*					
Data	Averaging	RELAX	M-RELAX	RELAX/M-RELAX($\tilde{P}=1$)	AR(order q)
34.540	16.051	14.516 ($P=1$)	14.323 ($P=1$)	12.402 ($P=1$)	14.512 ($q=2$)
		12.991 ($P=4$)	-9.597 ($P=4$)	11.068 ($P=4$)	
		12.235 ($P=7$)	-27.634 ($P=7$)	10.891 ($P=7$)	14.167 ($q=20$)
		11.927 ($P=10$)	-46.272($P=10$)	8.569 ($P=10$)	

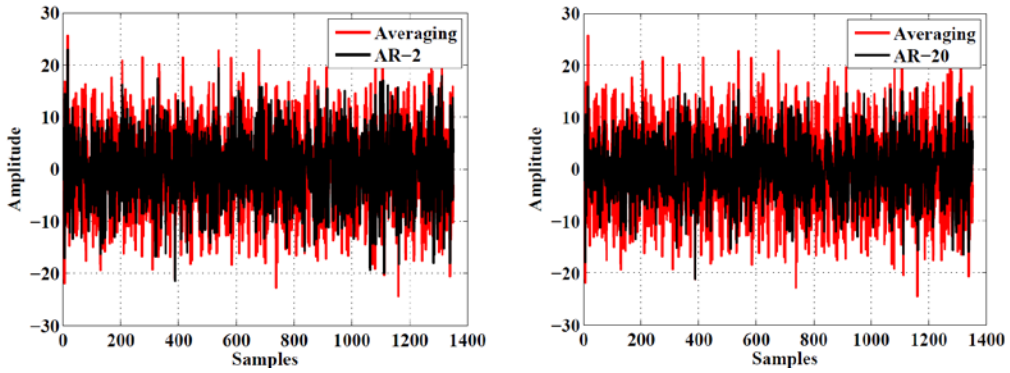

(a) (b)

FIG. 10 RFI SUPPRESSION–AR MODELINGWITHORDERqCOMPAREDTOAVERAGINGFOR "SNIFF" DATA (*File1*) (a) $q = 2$,AND (b) $q = 20$.

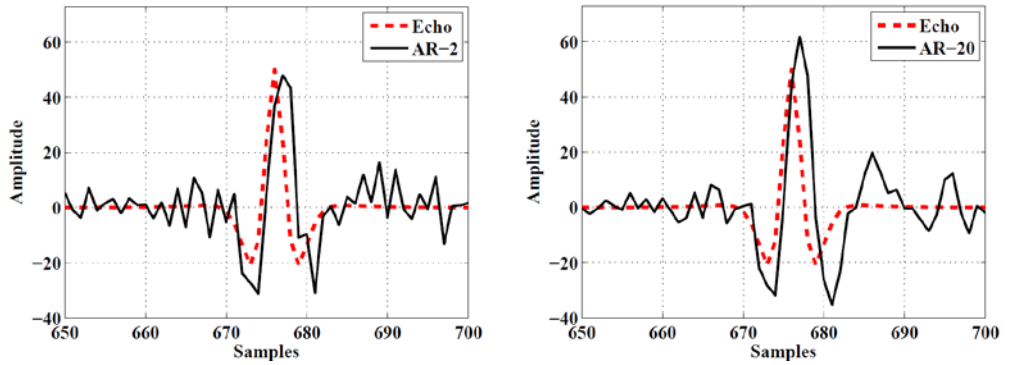

(a) (b)

FIG. 11ECHORETRIEVAL (*File1*)–AR MODELINGWITHORDERqCOMPARED TO IDEAL ECHOSIGAL (a) $q = 2$,AND (b) $q = 20$.

However, the target signatures are left basically unaltered as can be seen in Fig.8. Also in Table 5, the multi-snapshot RELAX algorithm shows a significant amount of suppression of the data as the number of sinusoids increases. Due to the issue of parameter identifiability discussed in the previous section, estimating more than $P = 2$ real-valued sinusoids, using only $N = 7$ real-valued samples per-snapshot will effectively suppress all the samples to zero. This leads to the suppression of the target energy, as it can also be seen in Fig. 8.

The multi-snapshot RELAX algorithm can be seen to improve on the suppression with little target distortion for $P = 1$.

This algorithm is combined with the RELAX algorithm to effectively suppress both wideband and narrowband interferers.

This improvement is seen in Table 5 and Fig. 9 shows the reconstructed echo after suppression. A similar analysis is performed for AR modelling. The AR modelling improves on the suppression compared to averaging as can be seen in Fig.10. However, this inverse filtering technique (see Appendix) leaves the desired signal distorted. This distortion is increased as the model order increases (due to filtering transients) as seen in Fig. 9. Hence the combined RELAX and multi-snapshot RELAX outperforms the AR approach in terms of both RFI suppression and desired target echo preservation.

Conclusions

In this paper, we have proposed a method for RFI suppression for the SIRE UWB radar, which is a cost efficient systemof sampling returned radar signals used for detecting landmines and IEDs developed by ARL. The low sampling rate and irregular sampling pattern of this radar poses a challenge for Radio Frequency Interference (RFI) suppression as the measured RFI signals will be severely aliased. In this paper,we have discussed the challenges of RFI suppression for this radar and proposed using the RELAX algorithm and its multi-snapshot counterpart as an intermediate step to the already proposed averaging scheme for RFI mitigation, for the SIREUWB radar. The results show that the RELAX algorithm can suppress RFI further, compared to averaging without altering desired target echo signals. The RELAX algorithms are easy to implement since they just involve FFTs. They have been shown to outperform AR modelling of the RFI signals.

The multi-snapshot RELAX uses a shorter time-duration (and fewer samples) for suppression, which yields a more accurate wideband model of the RFI assum of sinusoids compared to the RELAX algorithm. However, this algorithm significantly suppresses target signatures as the number of sinusoids increases and is limited to estimating only ones inusoid. Combining this algorithm assuming just one sinusoid, with the RELAX algorithm increases the suppression performance with little signal distortion.

ACKNOWLEDGMENT

The authors of this paper would like to thank the Army Research Laboratory for their support and also for providing us with the ”sniff” data set which was used for investigating RFI suppression.

REFERENCES

[1] Nehorai, D. Starer, and P. Stoica, “Direction-of-arrival estimation in applications with multipath and few snapshots,” Circuits, Syst., Signal Process., vol. 10, pp. 327–342, 1991.

[2] C. Li, J. Ling, J. Li, and J. Lin, “Accurate Doppler Radar Noncontact Vital Sign Detection Using the RELAX Algorithm,” IEEE Transactions on Instrumentation and Measurement, vol. 59, pp. 687 –695, March 2010.

[3] C. Yu, Y. Zhang, Z. Dong, and D. Liang, “Eigen-Decomposition Method for RFI Suppression Applied to SAR Data,” in Multimedia Technology (ICMT), 2010 International Conference on, pp. 1–4, oct. 2010.

[4] D. Vu, L. Xu, M. Xue, and J. Li, “Nonparametric Missing Sample Spectral Analysis and Its Applications to Interrupted SAR,” IEEE Journal of Selected Topics in Signal Processing, vol. 6, pp. 1–14, Feb. 2012.

[5] J. Li, D. Zheng, and P. Stoica, “Angle and waveform estimation via RELAX,” IEEE Transactions on Aerospace and Electronic Systems, vol. 33, pp. 1077–1087, July 1997.

[6] J. Li and P. Stoica, “Efficient Mixed-Spectrum Estimation with Applications to Target Feature Extraction,” IEEE Transactions on Signal Processing, vol. 44, pp. 281 –295, Feb. 1996.

[7] J. Li, P. Stoica, L. Xu, and W. Roberts, “On Parameter Identifiability of MIMO Radar,” IEEE Signal Processing Letters, vol. 14, pp. 968 –971, Dec. 2007.

[8] L. Nguyen, “Signal and Image Processing Algorithms for the U.S. Army Research Laboratory Ultra-wideband (UWB) Synchronous Impulse Reconstruction (SIRE) Radar,” ARL Technical Report, ARL-TR-4784, April 2009.

[9] L. Nguyen and M. Soumekh, “Suppression of Radio Frequency Interference (RFI) for Synchronous Impulse Reconstruction Ultra-Wideband Radar,” vol. 5808 of Proc. SPIE, pp. 178–184, 2005.

[10] L. Nguyen, M. Ressler, D. Wong, and M. Soumekh, “Adaptive Coherent Suppression of Multiple Wide-Bandwidth RFI Sources in SAR,” vol. 5427 of Proc. SPIE, pp. 1–16, 2004.

[11] L. Nguyen and R. Innocenti, “Suppression of sidelobes and noise in airborne SAR imagery using the Recursive Sidelobe Minimization technique,” in Radar Conference, 2010 IEEE, pp. 522 –525, May 2010.

[12] M. Braunstein, J. Ralston, and D. Sparrow, “Signal processing approaches to radio frequency interference (RFI) suppression,” in, Algorithms for Synthetic Aperture Radar Imagery, A. Giglio, eds., Orlando, FL, USA, vol. 2230, April 1994.

[13] M. Wax and I. Ziskind, “On unique localization of multiple sources by passive sensor arrays,” IEEE Transactions on Acoustics, Speech and Signal Processing, vol. 37, pp. 996 –1000, Jul. 1989.

[14] R. Lord and M. Inggs, “Approaches to RF Interference Suppression for VHF/UHF Synthetic Aperture Radar,” Proc. COMSIG, pp. 95–100,1998.

[15] R. Miles, A. Dogariu, and J. Michael, “Bringing bombs to light,” IEEE Spectrum, vol. 49, pp. 38 –43, February 2012.

[16] T. Miller, L. Potter, and J. McCorkle, “RFI Suppression for Ultra Wideband Radar,” IEEE Transactions on Aerospace and Electronic Systems, vol. 33, pp. 1142 –1156, Oct. 1997.

[17] P. Stoica, A. Jakobsson, and J. Li, “Cisoid parameter estimation in the colored noise case: asymptotic Cramer-Rao bound, maximum likelihood, and nonlinear least-squares,” IEEE Transactions on Signal Processing, vol. 45, pp. 2048 –2059, Aug. 1997.

[18] P. Stoica and R. L. Moses, Spectral Analysis of Signals. Upper Saddle River, NJ: Prentice-Hall, 2005.

[19] P. Stoica and Y. Selen, “Model-order selection: a review of information criterion rules,” IEEE Signal

Processing Magazine, vol. 21, pp. 36–47,July 2004.

[20] X. Huang and D. Liang, "Gradual RELAX algorithm for RFI suppressionin UWB-SAR," Electronics Letters, vol. 35, pp. 1916 –1917, Oct1999.

Appendix: AR Modelling for SIRE

Auto-regressive (AR) models, which is commonly used for modelling narrowband ("peaky") signals, can be used for estimating and suppressing RFI signals. The measured signal (RFI, desired target returns, and thermal noise) is modeled as an AR process [12]. The AR modelling (linear prediction modelling) equation is written as:

$$y[t_n] = -\sum_{i=1}^{q} a[i]y[t_n - i] + u[t_n] \qquad (21)$$

where, $y[t_n]$ is the measured data sequence, $u[t_n]$ corresponds to the white noise term at a time instant t_n and q corresponds to the AR order, which is determined by the number of spectral peaks and their widths. The assumption is that the first term on the right hand side of Eq. (21) corresponds to the RFI signal. The suppression process therefore involves estimating $\{a[i]\}_{i=1}^{q}$ and using the coefficients to suppress the RFI signals. Note that Eq. (21) can be re-written as:

$$y[t_n] = H(z)u[t_n] \qquad (22)$$

where $H(z) = 1/A(z) = 1/(1 + a[1]z^{-1} + \cdots + a[q]z^{-q})$ with z^{-1}being the delay operator. The RFI suppression process involves passing the measured data through the inverse filter $\frac{1}{H(z)} = \hat{A}(z)$ (from the estimated AR coefficients$\{\hat{a}[i]\}_{i=1}^{q}$).

The well-known methods for solving for the AR coefficients in (21) include the Yule-Walker (YW) method, Prony method and the modified Prony method [18]. The YW and Prony methods give similar results for large data samples. However, for smaller data records the Prony method tends to give more accurate AR estimates [18].

If both sides of the forward linear prediction equation (21) are multiplied by$y[t_n - t_m]$, and the expectation is taken, the well-known Yule-Walker equations are obtained.

$$\begin{bmatrix} r[1] \\ \vdots \\ r[n] \end{bmatrix} = \begin{bmatrix} r[0] & \cdots & r[-q+1] \\ \vdots & \ddots & \vdots \\ r[q] & \cdots & r[0] \end{bmatrix} \begin{bmatrix} a[1] \\ \vdots \\ a[q] \end{bmatrix} \qquad (23)$$

which can be re-written as $\mathbf{r} = -\mathbf{R}\mathbf{a}$. Where $\mathbf{r}$ and $\mathbf{R}$ are the covariance vecotr and matrix of the data. The AR coefficients ($\mathbf{a}$) are estimated by solving Eq. (23). The Yule-Walker method estimates the coefficients by replacing r with the standard biased autocorrelation sequence (ACS) estimator [18]. The Prony method solves the forward linear prediction equation (21) using least squares (LS). The problem reduces to (23), with the covariance sequence estimated by the standard unbiased ACS estimator [18].

The Modified Covariance (Prony) method (which improves on the Prony method) combines the forward linear prediction in (21) and the backward linear equation given in (24) to solve for the AR coefficients using least squares:

$$y[t_n] = -\sum_{i=1}^{q} a[i]y[t_n - i] + u[t_n] \qquad (24)$$

Where $a^b[i] = a[i]$. This *Modified Covariance Method* is applied to the SIRE sampled data which is sampled regularly in fast-time and slowtime. $N = 7$ sets of the slow-time regular samples ($K = 193$ samples per set) are used for AR modelling. The Modified Covariance equations can be written in matrix form as follows (for each set of slowtime samples):

$$\begin{bmatrix} y[q] \\ \vdots \\ y[K-1] \\ y[0] \\ \vdots \\ y[K-q-1] \end{bmatrix} = \begin{bmatrix} y[q-1] & \cdots & y[0] \\ \vdots & \ddots & \vdots \\ y[K-2] & \cdots & y[K-q-1] \\ y[1] & \cdots & y[q] \\ \vdots & \ddots & \vdots \\ y[K-q] & \cdots & y[K-1] \end{bmatrix} \begin{bmatrix} a[1] \\ a[2] \\ \vdots \\ a[q] \end{bmatrix} \qquad (25)$$

where q is the AR order. The equation can be re-written as $\mathbf{y}_n = -\mathbf{Y}_n \boldsymbol{a}$,for $n = 1,2,\ldots,N$ with $N = 7$.

The least-squares solution of this overdetermined linear system of equations is given by: $\mathbf{a} = -(\mathbf{Y}_n^T\mathbf{Y}_n)^{-1}(\mathbf{Y}_n^T\mathbf{y}_n)$ for $n = 1,2,\ldots,N$ with $N = 7$ where $(\mathbf{Y}_n^T\mathbf{Y}_n)^{-1}$ estimates the covariance matix $\mathbf{Y}_n^T\mathbf{y}_n$ estimates the ACS in (23). A more accurate estimate of the covariance matrixis derived from averaging $(\mathbf{Y}_n^T\mathbf{Y}_n)^{-1}$ for the $N = 7$ snapshots.

Ode Ojowu Jr. was born in Zaria, Nigeria in 1984. He received his B.Sc and M.Sc. degrees in electrical engineering from Washington University in St. Louis, St. Louis, Missouri, in 2007. He also received a B.A. in Physics from Grinnell College, Grinnell, Iowa in 2005. He is currently pursuing a Ph.D. degree in the

Department of Electrical and Computer in Engineering at the University of Florida, Gainesville, Florida.

His primary research interestests are in the areas of spectral estimation and array signal processing.

Jian Li, Dr. Jian Li received the M.Sc. and Ph.D. degrees in electrical engineering from The Ohio State University, Columbus, in 1987 and 1991, respectively.

From April 1991 to June 1991, she was an Adjunct Assistant Professor with the Department of Electrical Engineering, The Ohio State University, Columbus. From July 1991 to June 1993, she was an Assistant Professor with the Department of Electrical Engineering, University of Kentucky, Lexington. Since August 1993, she has been with the Department of Electrical and Computer Engineering, University of Florida, Gainesville, where she is currently a Professor. In Fall 2007, she was on sabbatical leave at MIT, Cambridge, Massachusetts. Her current research interests include spectral estimation, statistical and array signal processing, and their applications.

Dr. Li is a Fellow of IEEE and a Fellow of IET. She is a member of Sigma Xi and Phi Kappa Phi. She received the 1994 National Science Foundation Young Investigator Award and the 1996 Office of Naval Research Young Investigator Award. She was an Executive Committee Member of the 2002 International Conference on Acoustics, Speech, and Signal Processing, Orlando, Florida, May 2002. She was an Associate Editor of the IEEE Transactions on Signal Processing from 1999 to 2005, an Associate Editor of the IEEE Signal Processing Magazine from 2003 to 2005, and a member of the Editorial Board of Signal Processing, a publication of the European Association for Signal Processing (EURASIP), from 2005 to 2007. She has been a member of the Editorial Board of the IEEE Signal Processing Magazine since 2010 and a member of the Editorial Board of Digital Signal Processing - A Review Journal, a publication of Elsevier, since 2006. She is a co-author of the papers that have received the First and Second Place Best Student Paper Awards, respectively, at the 2005 and 2007 Annual Asilomar Conferences on Signals, Systems, and Computers in Pacific Grove, California. She is a co-author of the paper that has received the M. Barry Carlton Award for the best paper published in IEEE Transactions on Aerospace and Electronic Systems in 2005. She is also a co-author of the paper that has received the Lockheed Martin Best Student Paper Award at the 2009 SPIE Defense, Security, and Sensing Conference in Orlando, Florida.

Dr. Li is the director of the Spectral Analysis Lab (SAL) of the Department of Electrical and Computer Engineering at University of Florida.